Available online at www.sciencedirect.com
ScienceDirect
Journal of the European Ceramic Society 27 (2007) 3269–3275
www.elsevier.com/locate/jeurceramsoc

Development of ZrO_2–WC composites by pulsed electric current sintering

S.G. Huang, K. Vanmeensel, O. Van der Biest, J. Vleugels *

Department of Metallurgy and Materials Engineering, Katholieke Universiteit Leuven, Kasteelpark Arenberg 44, B-3001 Heverlee, Belgium

Received 2 September 2006; received in revised form 8 November 2006; accepted 20 November 2006
Available online 31 January 2007

Abstract

ZrO_2–WC ceramic composites with 40 vol% WC were consolidated by pulsed electric current sintering (PECS) for 4 min at 1450 °C under a pressure of 60 MPa. The effect of ZrO_2 stabilizers and the source of WC powder on the densification, phase constitution, microstructure and mechanical properties of the ZrO_2–WC composites were investigated and analyzed. The experimental results revealed that the amount and type of ZrO_2 stabilizers played a primary role on the phase constitution and mechanical properties of the composites in comparison to the morphology and size of the WC powder. The 2 mol% Y_2O_3-stabilized composites exhibited much better mechanical properties than that of 1.75 mol% Y_2O_3-stabilized or 1 mol% Y_2O_3 + 6 or 8 mol% CeO_2 co-stabilized composites. A Vickers hardness of 16.2 GPa, fracture toughness of 6.9 MPa $m^{1/2}$, and flexural strength of 1982 MPa were obtained for the composites PECS from a mixture of nanometer sized WC and 2 mol% Y_2O_3-stabilized ZrO_2 powder.

Keywords: ZrO_2; Carbides; Composites; SPS; Mechanical properties

1. Introduction

Tetragonal ZrO_2 polycrystals (TZP) are usually doped with Y_2O_3, CeO_2, CaO or other oxides to stabilize the high temperature tetragonal phase at room temperature. The transformation of tetragonal (t) to monoclinic (m) ZrO_2 phase contributes to the excellent mechanical properties such as high fracture toughness and bending strength. The application of structural ZrO_2 ceramics can be broadened by the incorporation of hard carbide inclusions in the TZP matrix, such as in TZP–SiC,[1,2] TZP–TiC[3] and TZP–WC[4–9] composites. Y_2O_3-stabilized TZP with WC addition was systematically investigated from the aspects of composition determination and sintering control.[6] Excellent combinations of hardness, fracture toughness and bending strength were obtained in hot pressed ZrO_2–40 vol% WC composites, which may partially replace the traditional WC–Co cemented carbides for some specific applications.[6,7]

In ZrO_2–WC composites, the mechanical properties can be modified both by the properties of WC and the ZrO_2 phases. A much higher hardness was obtained for composites with finer WC inclusions in comparison with coarse WC grains, even though the finer WC grades were more difficult to densify by hot pressing, and the fracture toughness of the composites is generally higher than for monolithic ZrO_2 ceramics.[6,7] In monolithic TZP materials, the t- to m-ZrO_2 phase transformation is a dominant toughening mechanism. The type and amount of stabilizers in ZrO_2 have a great impact on toughness. It can therefore be expected that the toughness of ZrO_2–WC composites can be manipulated by changing the type and amount of ZrO_2 stabilizers. Moreover, it has been reported that the hydrothermal stability and fracture toughness of Y–TZP can be improved by CeO_2 doping.[10,11] For hot pressed 2 mol% Y_2O_3-stabilized Y–TZP composites with up to 50 vol% WC addition, the best combination of toughness, hardness and strength was reported for ZrO_2 composites with 40 vol% WC addition.[6,7] For Y_2O_3 + CeO_2 co-stabilized ZrO_2 ((Y,Ce)–TZP), the optimum toughness was obtained with 1.0–1.5 mol% Y_2O_3 + 6–8 mol% CeO_2.[10,11]

The present study aimed to investigate the possibility to densify ZrO_2–WC composites by means of a very fast sintering technique, i.e. pulsed electric current sintering (PECS), which is also known as spark plasma sintering (SPS). The influence of

* Corresponding author. Tel.: +32 16 321244; fax: +32 16 321992.
E-mail address: Jozef.Vleugels@mtm.kuleuven.be (J. Vleugels).

0955-2219/$ – see front matter © 2006 Elsevier Ltd. All rights reserved.
doi:10.1016/j.jeurceramsoc.2006.11.079

Table 1
Starting powers used to make ZrO_2–40 vol% WC composites

Powder	Supplier	Grade	Powder size*
WC	MBN	J550	Agglomerates <10 μm; crystals <30 nm (XRD)
WC	ZhangYuan (ZY)	–	50 nm (XRD)
WC	OMG	Jet-milled	0.2 μm
WC	Eurotungstène	CW5000	0.8–1.0 μm
ZrO_2	Tosoh	TZ-0	27 nm
ZrO_2	Tosoh	TZ-3Y	30 nm
Y_2O_3	Atlantic Equipment Engineers	YT-603	–
$Ce(NO_3)_3{\cdot}6H_2O$	Aldrich Chemical company	–	–
Al_2O_3	Baikowski	SM8	0.8–1.0 μm

* Supplier data.

the size and morphology of the WC starting powder and the type and amount of ZrO_2 stabilizers on the mechanical properties of ZrO_2 composites with 40 vol% WC addition was investigated.

2. Experimental procedure

2.1. Materials preparation

ZrO_2–WC composites were prepared from three grades of nanometer sized and 1 μm sized WC powders with different morphologies and degree of agglomeration. The ZrO_2 matrix was stabilized with 1 mol% Y_2O_3 + 6 or 8 mol% CeO_2 (1Y6Ce or 1Y8Ce) prepared according to the powder coating technique.[11,12] Additionally, 1.75 and 2 mol% Y_2O_3-stabilized ZrO_2 (TM1.75 and TM2) were prepared by mixing commercial available 3Y–ZrO_2 and m-ZrO_2 powders. Additionally, 0.75 wt% Al_2O_3 was added to the ZrO_2–WC powder mixtures to assist sintering and limit ZrO_2 grain growth. Information on the starting powders is provided in Table 1.

To simplify the description, the composite grades are labelled as C1–C7, as listed in Table 2. The C1–C4 grades represent the composites composed of the nanometer sized MBN WC powder and the 1Y6Ce, 1Y8Ce, TM1.75 and TM2 ZrO_2 grades, which were selected to investigate the influence of the ZrO_2 composition on the composite properties. The composition of the ZrO_2 matrix was fixed to TM2, whereas the WC source was changed to ZY, OMG and CW5000 for the composite grade C5, C6 and C7 respectively. The powders were mixed in ethanol for 48 h on a multidirectional mixer (Turbula type) using WC–Co milling balls. The suspension was dried in a rotating evaporator at 80 °C.

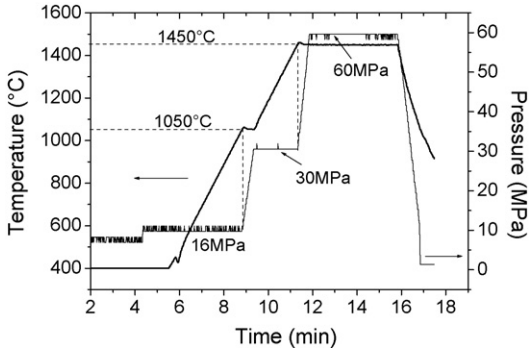

Fig. 1. PECS thermal and mechanical loading cycles to consolidate the ZrO_2–WC composites.

PECS (Type HP D 25/1, FCT Systeme, Rauenstein, Germany) was performed in a vacuum of 4 Pa. A pulsed electric current was applied with a pulse duration of 10 ms and pause time of 5 ms throughout all the experiments. The powder mixture (28.2 g) was poured into a cylindrical graphite die with an inner diameter of 30 mm and outer diameter of 66 mm and sintered for 4 min at 1450 °C under a maximum pressure of 60 MPa, with a heating and initial cooling rate of 200 °C/min. The thermal and mechanical loading cycles are shown in Fig. 1, in which the pressure was increased within 0.5 min from 16 to 30 MPa at 1050 °C, and adjusted within 0.5 min at 1450 °C from 30 to 60 MPa. Graphite paper was used to separate the

Table 2
Properties of the ZrO_2–40 vol% WC composites sintered at 1450 °C under a pressure of 60 MPa for 4 min

Grades	ZrO_2	WC	ρ (g/cm^3)	m/(m + t)[a] (vol%)	Δm[b] (vol%)	E (GPa)	HV_{10} (GPa)	K_{IC} (MPa.m$^{1/2}$)	TRS (MPa)
C1	1Y6Ce	MBN	9.75	32.2	32.1	369	14.9 ± 0.2	6.5 ± 0.1	816 ± 96
C2	1Y8Ce	MBN	9.80	40.7	20.0	369	14.7 ± 0.1	6.3 ± 0.2	884 ± 139
C3	TM1.75	MBN	9.66	42.3	22.2	378	14.4 ± 0.2	6.4 ± 0.2	1248 ± 57
C4	TM2	MBN	9.78	6.2	43.7	372	16.2 ± 0.1	7.3 ± 0.1	1873 ± 90
C5	TM2	ZY	9.76	6.1	47.6	360	16.0 ± 0.2	6.2 ± 0.1	1842 ± 70
C6	TM2	OMG	9.75	3.9	52.6	376	16.2 ± 0.2	7.0 ± 0.2	1982 ± 88
C7	TM2	CW5000	9.75	4.1	50.4	379	15.8 ± 0.1	7.3 ± 0.4	1914 ± 85
[c]ZrO_2	TM2	–	5.98	1.7	63.4	210	11.8 ± 0.1	6.5 ± 0.1	–

[a] Monoclinic ZrO_2 content.
[b] Δm: transformability of t-ZrO_2 phase.
[c] ZrO_2 obtained by PECS at 1450 °C for 2 min.

graphite die/punch set-up and powder mixture. Previous simulations, using a 40 mm diameter graphite die with 8.5 mm die wall thickness indicated a large radial temperature gradient >140 °C in case of a fully dense ZrO_2–40 vol% TiN composite sample, which was sintered at 1500 °C for 5 min.[13] In order to obtain a more homogeneous temperature distribution and concomitantly sintering behaviour, a 10 mm thick porous carbon felt insulation, minimizing the radiation heat losses from the outer die wall surface, was placed around the die, reducing the radial temperature gradient to 31 °C.[13] In order to obtain a realistic sample temperature measurement, a two-colour pyrometer (400–2300 °C, Impac, Chesterfield, UK) was focused at the bottom of a central borehole in the upper punch, just 2 mm away from the top surface of the sample. The sintered 4 mm thick disc-shaped samples were sand blasted, cross-sectioned and polished to 1 μm finish.

2.2. Characterization

The bulk density of the sintered composites was measured in ethanol. Phase identification was conducted by a θ–θ X-ray diffractometer (XRD, Seifert, Ahrensburg, Germany) using Cu Kα radiation (40 kV, 40 mA). The microstructure of the WC starting powders and the sintered composites were examined by scanning electron microscopy (SEM, XL30-FEG, FEI, Eindhoven, the Netherlands). The Vickers hardness, HV_{10}, was measured (Model FV-700, Future-Tech Corp., Tokyo, Japan) with an indentation load of 98.1 N. The fracture toughness, K_{IC}, was calculated from the length of the radial cracks of the indentations according to the formula proposed by Anstis et al.[14] The flexural strength at room temperature was measured in a three-point bending test (Series IX Automated Materials Testing System 1.29, Instron Corporation) on rectangular (25.0 mm × 2.9 mm × 1.8 mm) bars, which were cut by electrical discharge machining out of the sintered discs. All surfaces were ground with a Diamond Board MD40 75 B55 grinding wheel on a Jung grinding machine (JF415DS, Göppingen, Germany). The span width was 20 mm with a crosshead displacement of 0.1 mm/min. The elastic modulus, E, of the ZrO_2–WC composites was measured on the rectangular bars by the resonance frequency method.[15] The resonance frequency was measured by the impulse excitation technique (Grindo-Sonic, J.W. Lemmens N.V., Leuven, Belgium). The reported hardness, fracture toughness and flexural strength values are the mean and standard deviation of five measurements.

3. Results and discussion

3.1. WC starting powders and densification behaviour

SEM micrographs of the WC starting powders are shown in Fig. 2. The agglomerate size of the MBN grade (Fig. 2(a)) seems to be relatively larger compared to the other nanometer-sized ZY (Fig. 2(b)) and OMG (Fig. 2(c)) grades. The ZY and OMG grades are loosely agglomerated and show a quite homogeneous particle size distribution. The CW5000 grade is much coarser than the other powder grades, with an average particle size of about 0.8–1.0 μm.

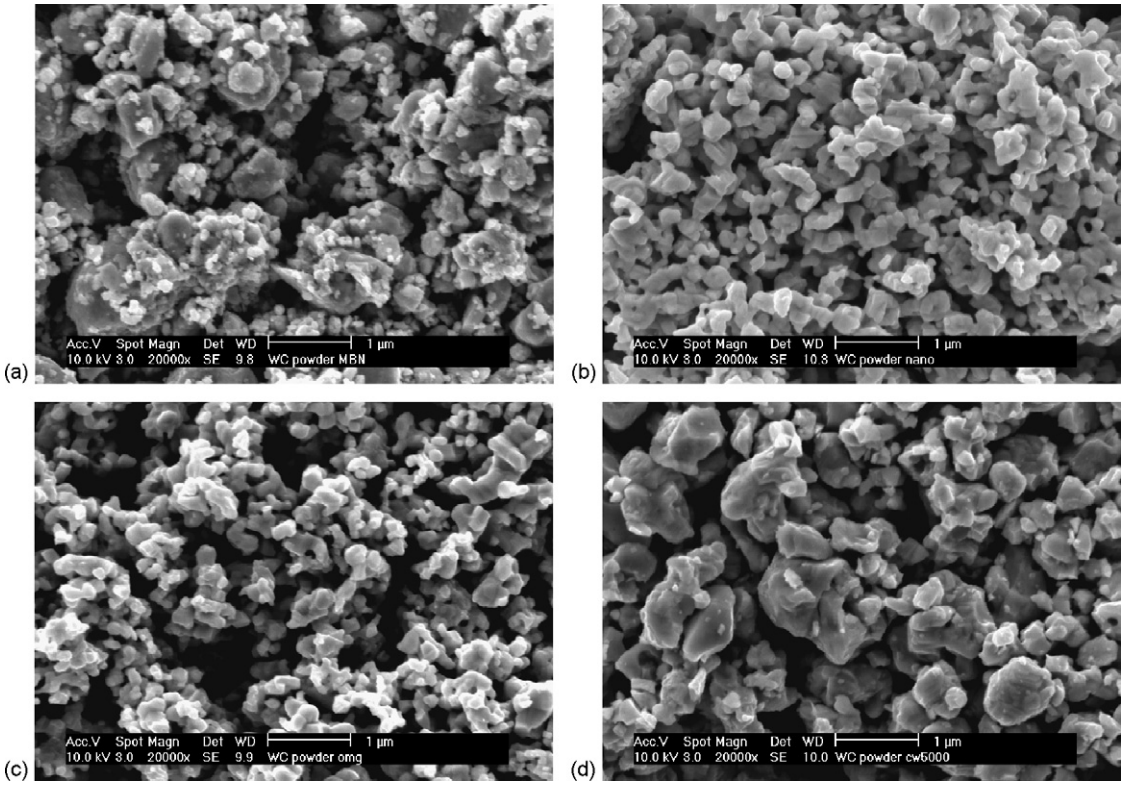

Fig. 2. Microstructure of the MBN (a), ZY (b), OMG (c) and CW5000 (d) WC starting powder grades.

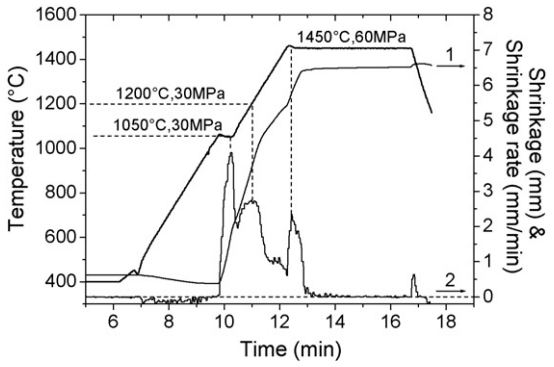

Fig. 3. Representative densification behaviour of the C4 grade ZrO_2–WC composite. The right axis contains the results of shrinkage (curve 1, mm) and shrinkage rate (curve 2, mm/min).

The density of the sintered composites is summarized in Table 2. Compared to a calculated theoretical density of 9.88 g/cm^3, nearly full densification was obtained for all composites, regardless of the WC source and the ZrO_2 powder compositions. During sintering, the densification behaviour of the ZrO_2–WC composites was automatically recorded from the displacement of the upper piston of the PECS equipment. Fig. 3 shows the representative densification behaviour of the C4 grade composite during the heating up and isothermal sections. The shrinkage started at 1050 °C upon increasing the pressure from 16 to 30 MPa. Rapid densification was achieved in the 1050–1450 °C range. Densification was nearly completed after dwelling for 1–2 min at 1450 °C under a pressure of 60 MPa.

Correspondingly, a few peaks were observed in the shrinkage rate curve during the heating-up stage. The peak at 1050 °C is correlated to particle rearrangement due to the increased pressure. The shrinkage peak at 1200 °C under a pressure of 30 MPa is mainly due to the densification of the ZrO_2 matrix phase. A maximum shrinkage rate was observed at 1260 °C for the pure TM2 ZrO_2 material grade when using the same thermal and mechanical loading cycles as for the composites. A fast shrinkage was observed at 1450 °C, when increasing the pressure from 30 to 60 MPa that could be correlated to the elimination of residual porosity. A similar shrinkage behaviour was observed for the other composites.

3.2. Constituent phases

The XRD patterns of the polished cross-sectioned MBN WC powder based ceramics with a 1Y6Ce, 1Y8Ce, TM1.75 and TM2 grade ZrO_2 matrix (composites C1–C4) composite surfaces are compared in Fig. 4, revealing that all composites exhibit the same phase constitution, i.e. t-ZrO_2 + WC + m-ZrO_2. The m- and t-ZrO_2 phase intensity of the PECS material grades however is different. Only a trace amount of m-ZrO_2 phase is observed on the polished C4 composite, whereas the other three composites exhibit a clear m-ZrO_2 peak. The WC powder source on the other hand hardly influenced the t-ZrO_2 phase stability, as revealed by the amount of m-ZrO_2 phase on polished surfaces of the C5, C6 and C7 composites in Table 2. These composites mainly consist of WC and t-ZrO_2 with a trace amount of m-ZrO_2.

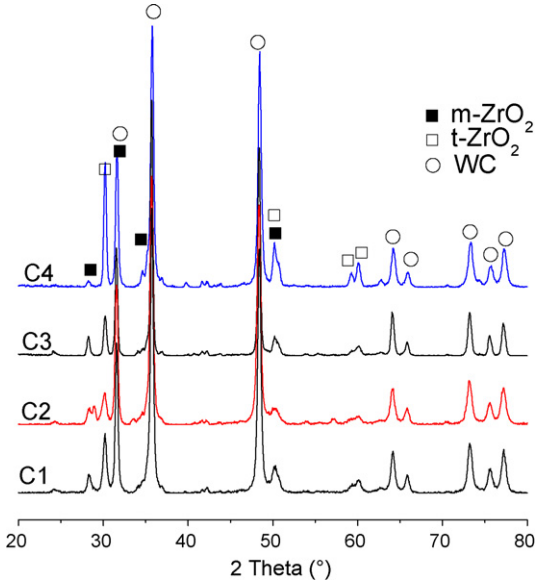

Fig. 4. XRD patterns of the MBN WC powder based ZrO_2–WC composites with 1Y6Ce (C1), 1Y8Ce (C2), TM1.75 (C3) and TM2 (C4) grade ZrO_2 powders.

The volume fraction of the m-ZrO_2 phase on the polished surface of the composites, measured and calculated according to method proposed by Toraya et al.,[18] is summarized in Table 2. It is clear that the MBN WC powder based composites with a TM1.75, 1Y6Ce and 1Y8Ce ZrO_2 matrix have a much higher amount of m-ZrO_2 phase compared to the composite with a TM2 ZrO_2 matrix. The presence of a large volume fraction of m-ZrO_2 phase on the polished surface at room temperature implies that the mechanical properties of the composites are degraded due to the presence of micro-cracks induced by the ZrO_2 phase transformation. The transformability, Δm of t-ZrO_2 phase in the composites, obtained from the difference in m-ZrO_2 phase content on fractured and polished surfaces is also included in Table 2. It should be clear that the t-ZrO_2 phase transformability of the composites with a TM2 ZrO_2 matrix is much higher than that of the composites with a 1.75 mol% Y_2O_3 or a mixed $Y_2O_3 + CeO_2$ stabilizer.

In general, a reduced stabilizer content leads to an enhanced t-ZrO_2 phase transformability and concomitant fracture toughness of Y–TZP ceramics, providing spontaneous transformation from t- to m-ZrO_2 is not initiated during cooling. In ZrO_2–WC composites however, the high level of thermal residual stresses due to the coefficient of thermal expansion mismatch between the WC and ZrO_2 phases also contribute to the lower stability of the t-ZrO_2 phase in the composites.[9] The residual tensile stress generated in the ZrO_2 phase due to the presence of the secondary WC phase during the fast cooling process results in a spontaneous phase transformation to m-ZrO_2 in the TM 1.75 ZrO_2 matrix composite, whereas the 2 mol% yttria stabilized composite is stable and almost fully tetragonal.

In a previous investigation, the t-ZrO_2 phase in monolithic 1Y6Ce and 1Y8Ce ceramics was shown to be stable after conventional pressureless sintering in air at 1450 °C for 1–4 h.[11] It is however known that CeO_2 is very sensitive to the sintering atmosphere and can be reduced to Ce_2O_3 when sintering in

vacuum, reducing or low oxygen pressure atmosphere. During PECS, a reducing environment is established due to the relatively high vacuum and the close contact of the ZrO_2 powder with the graphite die/punch set-up. The CeO_2 in solid solution is partially reduced to Ce_2O_3 during sintering, associated with an increase in the ionic radius from 0.101 nm for Ce^{4+} to 0.111 nm for Ce^{3+}. Ce_2O_3 is unstable in the ZrO_2 structure because of an approximately 40% mismatch in ionic radii of Ce^{3+} and Zr^{4+}, resulting in a decreased solubility of Ce_2O_3 in the t-ZrO_2 phase and segregation of Ce^{3+} to the grain boundaries,[16] which causes the destabilization of the t-ZrO_2 phase. The t-ZrO_2 phase in PECS monolithic 1Y6Ce and 1Y8Ce ceramics can however still be stabilized at room temperature because of the solution of 1 mol% Y_2O_3 in the t-ZrO_2 phase.[19] It is also possible to retain more t-ZrO_2 phase by decreasing the sintering temperature since the CeO_2 reduction is also dependent on the temperature.[17] For the ZrO_2–WC composites however, the reduction of CeO_2 in combination with the residual tensile stresses caused the high amount of m-ZrO_2 in the $Y_2O_3 + CeO_2$ co-stabilized ZrO_2–WC composites.

3.3. Microstructures

The microstructures of the MBN WC powder based composites are presented in Fig. 5. The white and grey contrast phases are respectively the WC and ZrO_2 phase. Elongated dark grains are observed in the CeO_2 co-stabilized C1 and C2 composites, which were identified as $CeAl_{11}O_{18}$ by EDS analysis. The formation of this phase clearly indicates the formation of Ce_2O_3 and the segregation of Al_2O_3 during sintering. In the yttria stabilized C3 and C4 composites, the dark Al_2O_3 grains are homogeneously distributed. The WC phase is mainly present as small agglomerates revealing that the deagglomeration of the WC starting powder is not complete after 48 h of multidirectional mixing.

The microstructures of the TM2 grade ZrO_2 composites with different WC sources are compared in Fig. 6. The white, grey and dark contrasts correspond to the WC, ZrO_2 and Al_2O_3 phases, respectively. A better distribution and finer WC grains can be observed in the ZY and OMG WC grade composites compared to the CW5000 grade composite, which is in agreement with the particle size distribution of the WC starting powders. The size of the WC phase in the MBN grade composite is comparable to that of the CW5000 grade, due to the rather strongly agglomerated nature of the nanocrystalline MBN powder caused by the mechanical milling preparation route. The angular shape WC particle size in the PECS ZY and OMG powder based composites is comparable and around 250 nm, whereas the CW5000 WC powder results in a composite with significantly larger rounded WC grains in the 1–2 μm range. As to the MBN grade composites, both the nanometer (<20 nm) and micrometer (>4 μm) sized WC particles can be observed, regardless of the source of ZrO_2 powders.

3.4. Mechanical properties

The mean and standard deviation of the Vickers hardness, toughness and three-point bending strength as well as E-moduli

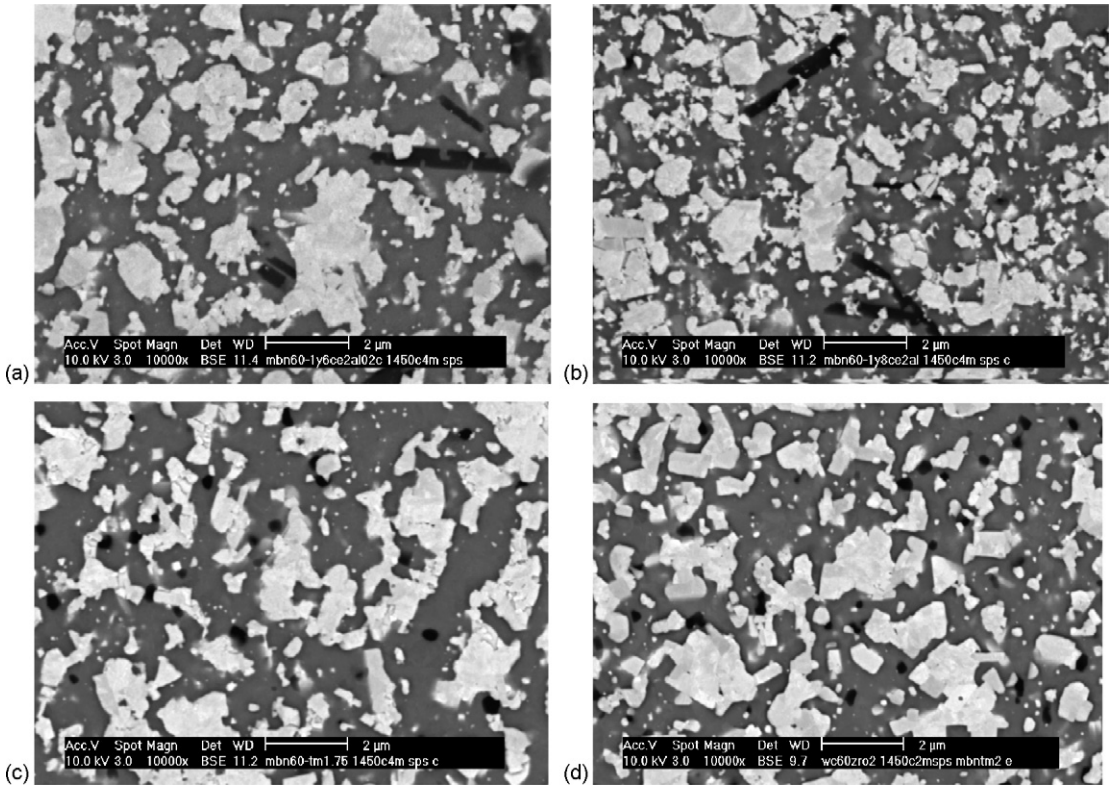

Fig. 5. Microstructures of the MBN WC powder based ZrO_2–WC composites, with a 1Y6Ce (C1), (a), 1Y8Ce (C2), (b), TM1.75 (C3), (c) and TM2 (C4), (d) ZrO_2 matrix.

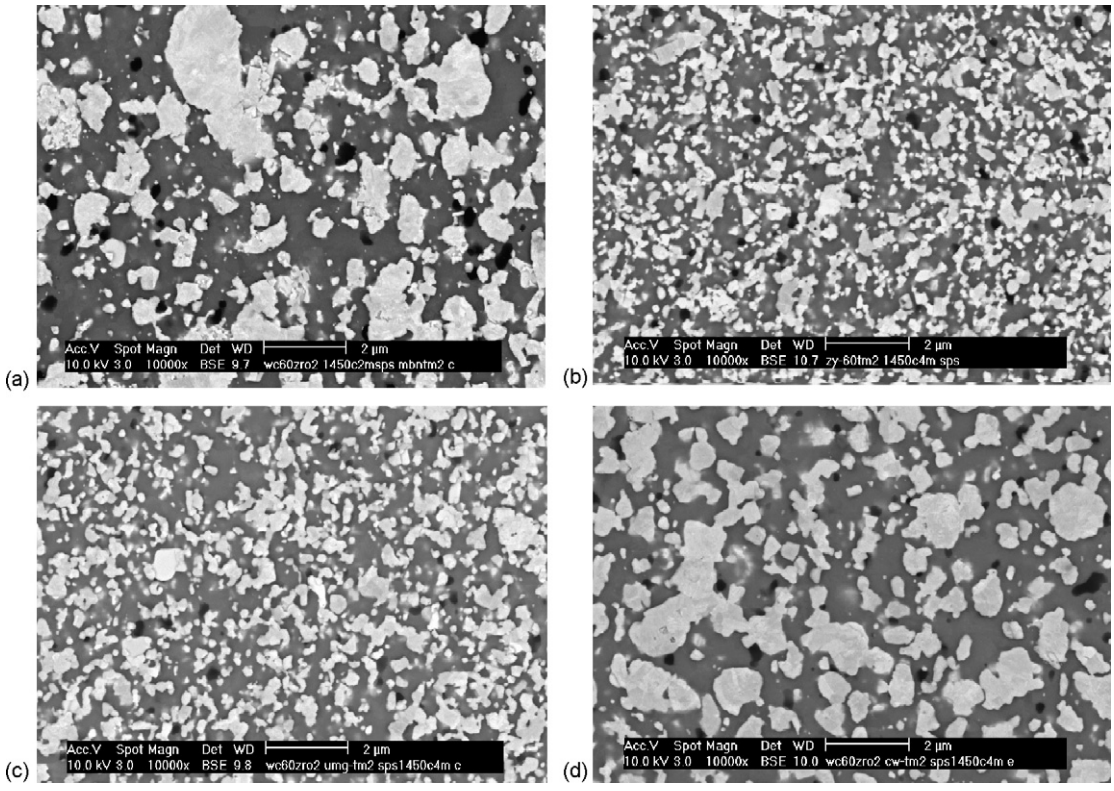

Fig. 6. Microstructures of the TM2 ZrO_2 powder based ZrO_2–WC composites, with MBN (C4), (a), ZY (C5), (b), OMG (C6), (c) and CW5000 (C7), (d) WC grade addition.

of the ZrO_2–WC composites are compared with that of a TM2 grade ZrO_2 in Table 2. All composites exhibit a much higher hardness than that of the monolithic ZrO_2, which can be explained by the harder WC inclusion, good coherence and chemical compatibility between WC and ZrO_2 components.[6] The hardness however is strongly influenced by the WC source as well as the ZrO_2 matrix. The t-ZrO_2 composites with low m-ZrO_2 content, composites C4–C7, have a significantly higher hardness, as shown in Table 2 and Fig. 7. The large amount of m-ZrO_2 in the other composites results in the formation of micro-cracks and a concomitantly lower hardness. The hardness of the ultra fine WC grained C4, C5 and C6 composites is slightly harder than that of the micrometer sized WC composite. When compared to hot pressed (1 h at 1450 °C) composites, the PECS (4 min at 1450 °C) composites exhibit a much higher hardness. For example, hot pressed CW5000 and MBN powder based ZrO_2–40 vol% WC composites have a hardness of 15.1 and 15.2 GPa,[7] whereas a hardness of, respectively, 15.8 and 16.2 is obtained by PECS.

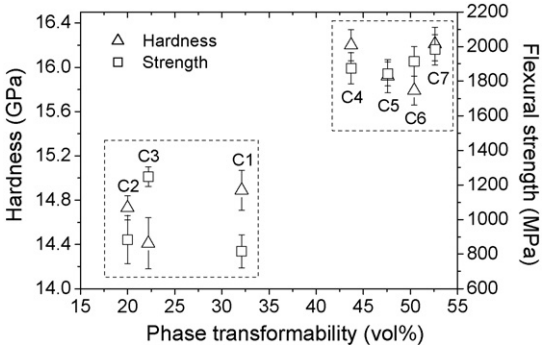

Fig. 7. Influence of the t-ZrO_2 phase transformability on the hardness and flexural strength of the ZrO_2–WC composites.

The effect of the m-ZrO_2 phase formation on the fracture toughness is not as significant as on the hardness. A fracture toughness of around 6.5 MPa $m^{1/2}$ was obtained for the high m-ZrO_2 content C1, C2 and C3 MBN WC powder based composites, which is comparable to that of the ZrO_2 ceramic but lower than for the t-ZrO_2 C4 composite. The toughness of the MBN, OMG and CW5000 WC powder based composites is comparable and around 7.0 MPa $m^{1/2}$. The toughness of the ZY WC powder based composite is lower and about 6.2 MPa $m^{1/2}$. For TZP ceramics, the stress-induced transformation plays an important role in the fracture toughness. Both t-ZrO_2 grain size and stabilizer content can affect the transformability of t-ZrO_2 phase and the concomitant toughness. The same is true for ZrO_2–WC composites, where the composite toughness is mainly determined by transformation toughening and crack deflection by the secondary WC phase.[6] As indicated in Table 2, the TM2 ZrO_2 based composites have a much higher transformability than the TM1.75, 1Y6Ce and 1Y8Ce composites, explaining their higher toughness. Despite the lower ZrO_2 phase transformability of the C1–C3 composites, the toughness is comparable to that of the ZrO_2 ceramic because of the crack deflection contribution of the secondary WC phase. Despite the lower t-ZrO_2 transformability, the toughness of the TM2 ZrO_2 composites is higher than that of the matrix material because of

the crack deflection contribution in the composites. The size of the WC phase influences the composite toughness. The crack deflection contribution to the toughness of the larger CW5000 WC grade or the larger MBN WC agglomerates is higher than that in the finer WC grained OMG and ZY WC powder based composites.

The flexural strength and hardness of the ZrO_2–WC composites is closely related, as illustrated in Fig. 7. The composites with higher t-ZrO_2 content and higher transformability clearly exhibit a higher flexural strength and hardness than the lower t-ZrO_2 content composites with a lower t-ZrO_2 transformability. An excellent flexural strength of 2000 MPa in combination with a hardness of 16.2 GPa was obtained for the TM2 based composites, which is about twice the strength of the 1Y6Ce, 1Y8Ce and TM1.75 ZrO_2 matrix composites. This reduction in strength and hardness can be explained by the presence of a large amount of m-ZrO_2 phase and concomitant micro-cracks.

The experimental findings reveal that the amount and transformability of the t-ZrO_2 phase determine the mechanical properties of ZrO_2–WC composites. To increase the transformability of the t-ZrO_2 phase, the amount and type of the stabilizer should be carefully selected as a function of the thermal sintering cycle. The hardness and toughness can only be slightly altered by controlling the morphology and size of the WC starting powders.

4. Conclusions

ZrO_2-based composites with 40 vol% WC addition could be fully densified by pulsed electric current sintering within 4 min at 1450 °C under a pressure of 60 MPa. The type and amount of ZrO_2 phase stabilizers strongly influence the microstructure and mechanical properties of the composites. 1.75 mol% Y_2O_3 stabilized and 1 mol% Y_2O_3 + 6 or 8 mol% CeO_2 co-stabilized ZrO_2–WC composites exhibited a lower amount of t-ZrO_2 phase with limited transformability, resulting in an acceptable hardness of 14.5 GPa, a toughness of 6.4 MPa $m^{1/2}$ and a flexural strength of 900 MPa.

An excellent combination of flexural strength, 2000 MPa, Vickers hardness, 16.2 GPa, and toughness of 6.9 MPa $m^{1/2}$ was obtained for the composites with a 2 mol% Y_2O_3 stabilized ZrO_2 matrix. The use of nano- or micrometer sized WC starting powder allowed to slightly adjust these mechanical properties. A larger WC grain or agglomerate size was found to slightly improve the fracture toughness.

Acknowledgements

This work was financially supported by the GROWTH program of the Commission of the European Communities under project contract no. G5RD-CT2002-00732 and the Research Fund K.U. Leuven under project GOA/2005/08-TBA.

References

1. Claussen, N., Weisskopf, K. L. and Rühle, M., Tetragonal zirconia polycrystals reinforced with SiC whiskers. *J. Am. Ceram. Soc.*, 1986, **69**, 288–292.
2. Poorteman, M., Descamps, P., Cambier, F., Leriche, E. and Thierry, B., Hot isostatic pressing of SiC-platelets/Y–TZP composites. *J. Eur. Ceram. Soc.*, 1993, **12**, 103–109.
3. Haberko, K., Pyda, W., Pêdzich, Z. and Bucko, M. M., A TZP matrix composite with in situ grown TiC inclusions. *J. Eur. Ceram. Soc.*, 2000, **20**, 2649–2654.
4. Pêdzich, Z., Haberko, K., Piekarczyk, J., Faryna, M. and Litynska, L., Zirconia matrix–tungsten carbide particulate composites manufactured by hot-pressing technique. *Mater. Lett.*, 1998, **36**, 70–75.
5. Haberko, K., Pêdzich, Z., Róg, G., Bucko, M. M. and Faryna, M., The TZP matrix–WC particulate composites. *Eur. J. Solid State Inorg. Chem.*, 1995, **32**, 593–601.
6. Anné, G., Put, S., Vanmeensel, K., Jiang, D., Vleugels, J. and Van der Biest, O., Hard, tough and strong ZrO_2–WC composites from nanosized powders. *J. Eur. Ceram. Soc.*, 2005, **25**, 55–63.
7. Jiang, D., Vleugels, J. and Van der Biest, O., ZrO_2–WC nanocomposites with superior properties. *J. Eur. Ceram. Soc.*, 2007, **27**, 1247–1251.
8. Pêdzich, Z., Haberko, K. and Faryna, M., Tetragonal zirconia–tungsten carbide composites manufacturing, microstructure and properties. In *Composites Science and Technology*, ed. S. Adali and V. Verijenko. University of Natal, South Africa, 1996, pp. 1–6.
9. Pêdzich, Z., Haberko, K., Faryna, M. and Sztwiertnia, K., Interphase boundary in zirconia–carbide particulate composites. *Key Eng. Mater.*, 2002, **223**, 221–226.
10. Lin, J.-D. and Duh, J.-G., Correlation of mechanical properties and composition in tetragonal CeO_2–Y_2O_3–ZrO_2 ceramic system. *Mater. Chem. Phys.*, 2003, **78**, 246–252.
11. Huang, S. G., Vleugels, J., Li, L., Van der Biest, O. and Wang, P. L., Composition design and mechanical properties of mixed (Ce,Y)–TZP ceramics obtained from coated starting powders. *J. Eur. Ceram. Soc.*, 2005, **25**, 3109–3115.
12. Vleugels, J., Yuan, Z. X. and Van der Biest, O., Mechanical properties of Y_2O_3/Al_2O_3-coated Y–TZP ceramics. *J. Eur. Ceram. Soc.*, 2002, **22**, 873–881.
13. Vanmeensel, K., Laptev, A., Van der Biest, O. and Vleugels, J., Field assisted sintering of electro-conductive ZrO_2-based composites. *J. Eur. Ceram. Soc.*, 2007, **27**, 979–985.
14. Anstis, G. R., Chantikul, P., Lawn, B. R. and Marshall, D. B., A critical evaluation of indentation techniques for measuring fracture toughness: I. Direct crack measurements. *J. Am. Ceram. Soc.*, 1981, **64**, 533–538.
15. ASTM E 1876-99. Standard test method for dynamic young's modulus, shear modulus, and poisson's ratio for advanced ceramics by impulse excitation of vibration. *ASTM Annual Book of Standards*. Philadelphia, PA; 1994.
16. Hwang, S. L. and Chen, I.-W., Grain size control of tetragonal zirconia polycrystals using the space charge concept. *J. Am. Ceram. Soc.*, 1990, **73**, 3269–3277.
17. Huang, S. G., Li, L., Van der Biest, O. and Vleugels, J., Influence of the oxygen partial pressure on the reduction of CeO_2 and CeO_2–ZrO_2 ceramics. *Solid State Sci.*, 2005, **7**, 539–544.
18. Toraya, H., Yoshimura, M. and Somiya, S., Calibration curve for quantitative analysis of the monoclinic-tetragonal ZrO_2 system by X-ray diffraction. *J. Am. Ceram. Soc.*, 1984, **67**, C119–C121.
19. Huang, S. G., Vanmeensel, K., Van der Biest, O. and Vleugels, J., Influence of CeO_2 reduction on the microstructure and mechanical properties of pulsed electric current sintered Y_2O_3–CeO_2 co-stabilized ZrO_2 ceramics, *J. Am. Ceram. Soc.*, in press.